

Regulation of Constitutive Exocytic Transport by Membrane Receptors

A BIOCHEMICAL AND MORPHOMETRIC STUDY*

(Received for publication, August 3, 1995, and in revised form, October 12, 1995)

Roberto Buccione‡§, Sergei Bannykh¶, Ivana Santone||, Massimiliano Baldassarre||, Francesco Facchiano, Yuri Bozzi**, Giuseppe Di Tullio, Alexander Mironov, Alberto Luini, and Maria Antonietta De Matteis||

From the Istituto di Ricerche Farmacologiche Mario Negri, Consorzio Mario Negri Sud, Laboratory of Molecular Neurobiology and the ||Physiopathology of Secretion Unit, 66030 S. Maria Imbaro (Chieti), Italy

Biochemical and morphometric approaches were combined to examine whether constitutive secretory transport might be controlled by plasma membrane receptors, as this possibility would have significant physiological implications. Indeed, IgE receptor stimulation in rat basophilic leukemia cells potently increased the rate of transport of soluble pulse-labeled ³⁵S-sulfated glycosaminoglycans from distal Golgi compartments to the cell surface. This effect was largely protein kinase C (PKC)-dependent. Direct activation of PKC also stimulated constitutive transport of glycosaminoglycans, as indicated by the use of agonistic and antagonistic PKC ligands. PKC ligands also had potent, but different, effects on the exocytic transport from distal Golgi compartments to the plasma membrane of a membrane-bound protein (vesicular stomatitis virus glycoprotein), which was slightly stimulated by activators and profoundly suppressed by inhibitors of PKC. Morphological analysis showed impressive changes of the organelles of the secretory pathway in response to IgE receptor stimulation and to direct PKC activation (enhanced number of buds and vesicles originating from the endoplasmic reticulum and Golgi and increase in surface and volume of Golgi compartments), suggestive of an overall activation of exocytic movements. These results show that rapid and large changes in constitutive transport fluxes and in the morphology of the exocytic apparatus can be induced by membrane receptors (as well as by direct PKC stimulation).

Constitutive membrane transport is fundamental to a number of cellular functions including growth and differentiation, secretion of proteins such as immunoglobulins, proteoglycans, serum, matrix, and milk proteins, as well as generation, homeostasis, and turnover of cellular organelles. Such essential functions are likely to be precisely controlled.

Certain basic steps in membrane and protein transport such as vesicle formation, docking, and fusion have been studied extensively over the last decade, and a fundamental set of molecular mechanisms executing these events has been elucidated (1). Superimposed on this core machinery, regulatory mechanisms must exist to fine tune membrane traffic, maintain organelle homeostasis, and mediate adaptive responses of transport to variations in extracellular conditions. In spite of their potentially great physiologic importance, however, they have received relatively little attention.

Evidence has nevertheless accumulated showing that regulatory molecules play a role in constitutive membrane traffic. Heterotrimeric GTP-binding proteins have been implicated in the secretion of proteoglycans (2), apical secretion in polarized cells (3), endosome-endosome fusion (4), transcytosis (5, 6), in the association of coatamer with Golgi membranes (7), vesicle formation from the distal Golgi (8), and ER¹ to Golgi transport (9). Protein phosphorylation has been shown to be involved in the regulation of traffic; ER to Golgi transport is suppressed by protein phosphatase inhibitors (10). Vesicle formation from the trans Golgi/trans Golgi network (TG/TGN) is dependent on protein phosphorylation (11); hyperphosphorylation of a yet unidentified protein(s) leads to a block of homologous endosome fusion *in vitro* (12); the mitotic kinase Cdc2 has also been proposed to be responsible for the endosome fusion block at mitosis (13).

On the basis of these considerations, we have recently investigated the possibility that signal transduction pathways might control constitutive membrane traffic and reported that protein kinase C (PKC) and PKC-coupled receptors modulate the association of ADP-ribosylation factor (ARF) to the Golgi apparatus (14). ARF binding to Golgi membranes is a key molecular step in vesicular traffic (1). This finding has helped bring into focus the link between constitutive traffic and signal transduction and further stimulated interest in the question as to whether segments of the membrane traffic pathways may be regulated by second messengers (15) and by which mechanisms. Most recently, a number of reports have produced evi-

* This work was supported in part by the Italian National Research Council (Convenzione CNR-Consorzio Mario Negri Sud). The costs of publication of this article were defrayed in part by the payment of page charges. This article must therefore be hereby marked "advertisement" in accordance with 18 U.S.C. Section 1734 solely to indicate this fact.

‡ To whom correspondence should be addressed: Laboratory of Molecular Neurobiology, Consorzio Mario Negri Sud, 66030 S. Maria Imbaro (Chieti), Italy. Tel.: 39-872-570354; Fax: 39-872-578240.

§ Recipients of a postdoctoral fellowship from the Ministero del Lavoro-POFSE 936106 I1 "Esperto in tecnologie farmacologiche e biomediche avanzate nel campo della ricerca farmaceutica e agroalimentare."

¶ Present address: Depts. of Cell and Molecular Biology, The Scripps Research Inst., La Jolla, CA 92037.

** Present address: Laboratorio di Biologia Cellulare e dello Sviluppo, Università di Pisa, Via Carducci 13, 56010 Ghezzano (PI) Italy.

¹ The abbreviations used are: ER, endoplasmic reticulum; PKC, protein kinase C; TG/TGN, trans Golgi/trans Golgi network; ARF, ADP-ribosylation factor; RBL, rat basophilic leukemia; BFA, brefeldin A; PMA, phorbol 12-myristate 13-acetate; DNP, dinitrophenol; BSA, bovine serum albumin; DPP, 12-deoxyphorbol 13-phenylacetate; DPPA, 12-deoxyphorbol 13-phenylacetate 20-acetate; VSV, vesicular stomatitis virus; MEM, Eagle's minimal essential medium; DMEM, Dulbecco's modified Eagle's medium; FCS, fetal calf serum; PAGE, polyacrylamide gel electrophoresis; GAG, free glycosaminoglycan chains; VSV-G, VSV glycoprotein; PBS, phosphate-buffered saline; MCV, mean cell volume; MAC₁, mean area of cell projections; MAC₂, mean area of cell sections; TVC, tubular-vesicular clusters; DAG, diacylglycerol.

dence that, indeed, diverse transport pathways can be affected by bacterial toxins or drugs modifying the level of second messengers (16–21).

To assess the physiological significance of these regulatory phenomena, we have studied the effects of receptor stimulation on constitutive membrane traffic. Biochemical analysis indicates that in RBL cells, the IgE receptor can control membrane and solute exocytic fluxes from the TG/TGN to the cell surface mostly via PKC. Morphological analysis extends this observation, revealing changes of the secretory apparatus (enhanced number of buds and vesicles originating from both the ER and the Golgi complex, and increase in surface and volume of Golgi compartments), suggestive of an overall acceleration of exocytic transport. The results suggest that signal transduction systems can play a crucial role in the mechanisms controlling size and transport activity of the exocytic organelles.

EXPERIMENTAL PROCEDURES

Materials—Ro 31-8220 was a gift from Roche Research Centre (Wellwyn Garden City, UK). Brefeldin A (BFA), phorbol 12-myristate 13-acetate (PMA), streptavidine-agarose, mouse anti-dinitrophenol (DNP) IgE, horseradish peroxidase type II, *p*-nitrophenyl β -D-xylopyranoside (xyloside), and adenosine 3'-phosphate 5'-phosphosulfate were purchased from Sigma; NHS-LC-biotin was from Pierce (Rockford IL). Calphostin C, DNP-bovine serum albumin (BSA) conjugate (DNP-BSA), and A23187 were from Calbiochem (San Diego, CA). 12-Deoxyphorbol 13-phenylacetate (DPP), 12-deoxyphorbol 13-phenylacetate 20-acetate (DPPA), and thymeleatoxin were purchased from LC Laboratories (Woburn, MA). Cell culture media and sera were from Life Technologies, Inc. and Seromed (Berlin, Germany). Tran³⁵S-label (a mixture of ³⁵S-labeled methionine and cysteine) was purchased from ICN (Irvine, CA). [³H]Hydroxytryptamine (serotonin) binoxalate was from E. I. du Pont de Nemours (Cologno Monzese, Italy). [³⁵S]Sulfate was from Amersham Corp. All other reagents were of the best available quality from various sources. The ts045 temperature mutant of vesicular stomatitis virus (VSV) was a generous gift of Dr. K. Simons (EMBL, Heidelberg, Germany).

Cell Culture—RBL cells were grown in Eagle's minimal essential medium (MEM) supplemented with 16% fetal calf serum (FCS) and 1 mM L-glutamine; PC12 cells were grown Dulbecco's modified Eagle's medium (DMEM) containing 10% heat-inactivated horse serum and 5% FCS. Madin-Darby canine kidney cells, obtained from Dr. M. Cardone (University of California, San Francisco CA), were cultured in DMEM with 10% FCS; HL-60 cells were grown in RPMI with 10% FCS.

Analysis of Proteoglycan and Free Glycosaminoglycan Chain Release by SDS-PAGE—Cells at confluence (80% for PC12 cells) in 6-well plates (plated 24 h before the experiment) were washed with Tyrode's solution (Tyrode: 125 mM NaCl, 5 mM KCl, 5.6 mM glucose, and 20 mM Hepes-NaOH, pH 7.2) containing 1.8 mM each CaCl₂ and MgCl₂ (Tyrode/Ca+Mg) and incubated 15 min at 37 °C in 1 ml of the same buffer with or without 1 mM xyloside to label free glycosaminoglycan chains (GAG) or proteoglycans, respectively. The buffer was then substituted with 0.6 ml of Tyrode/Ca+Mg containing 80–150 μ Ci/ml [³⁵S]sulfate, and the incubation continued for 5 min at 37 °C. Cells were washed with serum-free MEM and then incubated in 0.6 ml of the same medium for varying times with or without the various treatments. Samples were prepared for SDS-PAGE according to Brion *et al.* (22) with some modifications. The release medium from each sample was precipitated overnight in 80% acetone and 20 μ g of chondroitin sulfate as a carrier at –20 °C. Precipitates were pelleted at 27,000 \times g for 30 min and boiled in Laemmli (23) sample buffer for 5 min. Cell extracts were prepared by adding 80 μ l of sample buffer directly to the culture well and boiling for 60 min. Samples were subjected to SDS-PAGE on 5–20% gradient gels. Finally, gels were dried and quantified by electronic autoradiography on a Packard InstantImager or exposed to Kodak X-Omat AR film.

Analysis of Proteoglycan and GAG Release by Cetylpyridinium Chloride Precipitation—Cells at confluence (80% for PC12 cells) in 12-well plates (plated 24 h before the experiment) were washed, incubated with or without xyloside, labeled with [³⁵S]sulfate, and treated for release as described above with the addition of 0.1% BSA. Release media were collected and centrifuged (12,000 \times g for 10 min), and the supernatant was recovered. Cell monolayers were extracted with 0.5 ml of 0.1 M NaOH for at least 30 min at 37 °C. ³⁵S-Labeled proteoglycans or GAG were quantified by a precipitation assay as described previously (24) with minor modifications. Briefly, cell supernatants and extracts (0.5

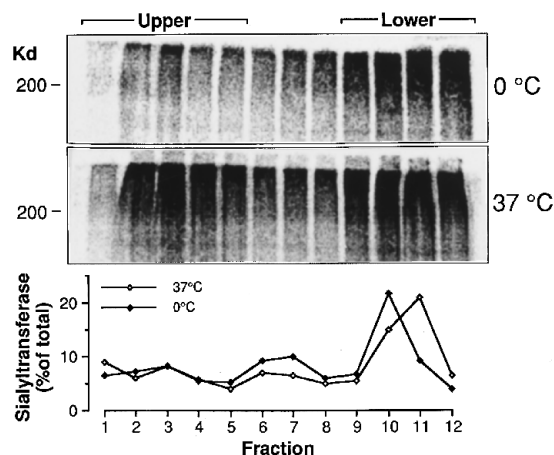


FIG. 1. Cell-free formation of secretory vesicle from the TG/TGN in PC12 cells. A postnuclear supernatant from PC12 cells pre-labeled with [³⁵S]sulfate, was incubated at 37 °C to allow vesicle formation *in vitro*. After the reaction, the suspension was centrifuged on a continuous sucrose gradient to separate small vesicles (*upper fractions*) from larger membranes (*lower fractions*). Fractions were analyzed by SDS-PAGE, and radioactivity was quantified with an InstantImager. The distribution of labeled proteoglycans between upper and lower fractions (from fraction 1 to 12) is shown for a sample incubated for 30 min at 37 °C and a control sample incubated for the same time at 0 °C. The distribution of sialyltransferase activity across the gradient is also shown for samples incubated at 0 °C (filled symbols) and at 37 °C (empty symbols). The ratio between radioactivity in the upper versus lower fractions is taken as an index of vesicle formation from the TG/TGN (see Table III).

ml) were precipitated overnight at room temperature by the addition of chondroitin sulfate (0.6% final concentration) and cetylpyridinium chloride (1% final concentration). Precipitates were collected by centrifugation (2600 \times g for 10 min) and washed twice with 1% cetylpyridinium chloride in 20 mM NaCl. Finally, pellets were dissolved in 2 M NaCl at 37 °C and radioactivity measured in a scintillation counter using Beckman Ultima Gold XR.

Analysis of Regulated Release of Serotonin from RBL Cells—The release of serotonin from secretory granules in RBL cells was measured as follows. Cells at confluence in 24-well plates were labeled with 1 μ Ci/ml [³H]serotonin the day before the experiment. Cells were washed with Tyrode, and release, in response to various agonists, was assayed exactly as described in Ref. 25.

Cell-free Vesicle Formation and Subcellular Fractionation—Cell-free vesicle formation was carried out as described by Tooze and Huttner (26). Briefly, PC12 cells (2 \times 15-cm dishes at 80% confluence/sample) were starved for 30 min at 37 °C in 10 ml of labeling DMEM (DMEM lacking bicarbonate and sulfate with only 1% of the normal methionine and cysteine concentrations and containing 10 mM Hepes, pH 7.4) supplemented with 1% dialyzed horse serum and 0.5% dialyzed FCS. This was substituted with 4 ml of fresh labeling DMEM containing 350 μ Ci/ml [³⁵S]sulfate, and the incubation continued for 4.5 min. Next, a postnuclear supernatant was prepared from the labeled cells as follows. Cells were scraped and homogenized with a cell cracker (EMBL workshop, Heidelberg Germany) on ice at a 18- μ m clearance in HBS (0.25 M sucrose, 1 mM EDTA, 1 mM magnesium acetate, 1.6 mM Na₂SO₄, 10 mM Hepes-KOH, pH 7.2). The resulting postnuclear supernatant was incubated at 37 °C, from 15 to 60 min, in the presence of adenosine 3'-phosphate 5'-phosphosulfate, ATP, and an ATP-regenerating system, with or without the various agonists or inhibitors. The control sample was incubated at 0 °C. After incubation, samples were subjected for 15 min at a 80,000 \times g velocity gradient centrifugation on a linear 0.3/1.2 M continuous sucrose gradient. 12 1-ml fractions were collected and precipitated overnight with 10% trichloroacetic acid containing 1 mg/ml sodium deoxycholate or assayed for sialyltransferase activity, as described in Ref. 27. Precipitates were recovered by centrifugation at 12,000 \times g for 15 min, washed twice with cold acetone, resuspended in 60 μ l of sample buffer, and boiled 5 min. Electrophoresis was carried out on 5–10% gradient acrylamide gels. Finally, gels were dried and quantified on a Packard InstantImager or exposed to Kodak X-Omat AR film. Fig. 1 shows the distribution of ³⁵S-labeled proteoglycans between upper and lower fractions at 0 and 37 °C. The formation of vesicles *in*

vitro, as measured by the shift of labeled proteoglycans from the lower into the upper fractions, as compared with the 0 °C control (26), occurred rather efficiently in basal conditions; it was independent of the presence of Ca^{2+} and reached a plateau at 30–60 min (60 min not shown). The shift of labeled material from lower to upper fractions was very likely due to active vesicle formation rather than damage (fragmentation) of the Golgi membranes since the profile of the resident trans Golgi marker sialyltransferase was not significantly changed by the different treatments (Fig. 1). The small amount of labeled material present in upper fractions in the 0 °C sample is most probably due to some degree of TGN fragmentation and/or to the formation of transport vesicles *in vivo* prior to homogenization.

VSV Infection and Assay of VSV Glycoprotein (VSV-G) Transport by Cell Surface Biotinylation—RBL cells were plated at confluence in 12-well plates and infected the following day at 31 °C with the ts045 mutant (28) of VSV in MEM containing 10% FCS and 5 $\mu\text{g}/\text{ml}$ actinomycin D. 1 h later, the medium was replaced with MEM, and the incubation continued for an additional 2 h. To label proteins, cells were starved 10 min at the nonpermissive temperature of 40 °C in DMEM lacking methionine and cysteine, pulse-labeled with [^{35}S]methionine (50–60 $\mu\text{Ci}/\text{ml}$) for 10 min at 40 °C, and then shifted to 19.5 °C for 2 h (to block proteins in the TGN) in complete MEM supplemented with 2 mM methionine. The cells were then incubated at 37 °C with or without agonists for various times. A control was performed by incubating cells at 0 °C. Cell surface proteins were biotinylated according to Refs. 29 and 30. Briefly, after washing in phosphate-buffered saline (PBS/Ca+Mg) (PBS containing 0.1 mM each CaCl_2 and MgCl_2), cells were incubated on ice twice with NHS-LC-biotin (0.5 mg/ml in PBS/Ca+Mg) for 20 min, quenched 2×15 min with PBS containing 50 mM NH_4Cl , and extensively washed with PBS/Ca+Mg. Biotinylated cells were lysed for 60 min in lysis buffer (150 mM NaCl, 20 mM Tris pH 9, 5 mM EDTA, 1% Triton X-100, 0.2% BSA). Material from two wells was collected and centrifuged 10 min at $14,000 \times g$, and aliquots of the supernatant were precipitated with trichloroacetic acid or incubated overnight at 4 °C with 30 μl of a streptavidin-agarose bead suspension. The beads were centrifuged at $14,000 \times g$ for 30 s and washed extensively with TBS containing 1% Triton X-100. Bound material was eluted from the beads with 100 μl of Laemmli sample buffer after three rounds of 5 min each of stirring and boiling (fresh 2-mercaptoethanol was added after each boiling to a final concentration of 5% (v/v)). The eluted material was analyzed by 8% acrylamide SDS-PAGE. Finally, gels were dried and quantified on a Packard InstantImager or exposed to Kodak X-Omat AR film.

Transmission Electron Microscopy—Cells were grown on Thermanox coverslips (Nunc Inc., Illinois) to 80% confluence, fixed with 2.5% glutaraldehyde in 10 mM PBS for 12 h, post fixed in 1% buffered OsO_4 for 1 h, stained en bloc in 1% uranyl acetate, and embedded in Epon 812. Ultrathin sections were stained with uranyl acetate and lead citrate and photographed with a Zeiss 109 transmission electron microscope.

Morphometry—All stereological values in this study are related to the mean cell volume (MCV) taken as a reference space. MCV was measured by two independent methods to control for possible errors inherent in each technique. The first was based on the estimation of the mean surface and height of cells grown in monolayers (31, 32). Briefly, after glutaraldehyde fixation, cells were viewed and photographed in phase contrast under an Axiophot microscope (Zeiss, Germany) with a $20\times$ objective lens. The images were photographically enlarged 10 times, and the mean area of cell projections (MAC_1) was determined by the point counting method (33) using 5-mm-square lattice grids. No less than 2×10^3 RBL cells were used for each time point. Cells on coverslips were then stained and embedded in Epon as described above and detached by immersion in liquid nitrogen, and two square pieces of Epon layers were sandwiched together, re-embedded in Epon, and cut along a plane perpendicular to the monolayers to produce vertical sections (31). Thin sections were viewed at the electron microscope and photographed at a $3500\times$ final magnification. Cell heights were determined by the semiautomatic image analyzer Videoplan 2 (Zeiss, Germany) by precisely tracing cellular contours with the cursor on the digitizing tablet and were used to calculate mean cell height (H_c). MCV was determined according to the formula $\text{MCV} = \text{MAC}_1 \cdot H_c$. No less than 95 RBL cells contours were used to evaluate H_c for each time point of PMA treatment. The second method was used to estimate the MCV in cells in suspension. Cells were grown on tissue culture dishes, fixed in 2.5% glutaraldehyde, scraped, spun down, and processed for electron microscopy. The mean area of cell sections (MAC_2) was determined by Videoplan 2, and the MCV was determined by the formula: $\text{MCV} = 1.4(\text{MAC}_2)^{3/2}$, where 1.4 is a coefficient related to the cell shape (33). No less than 100 cells were used per treatment. The MCVs of RBL cells

TABLE I
Basic stereological estimations of RBL cells

	Cell	Nucleus	Endoplasmic reticulum	Golgi complex
Volume (μm^3)	780 ^a	217 \pm 12	36 \pm 2	7 \pm 0.5
Surface (μm^2)	655 \pm 27	176 \pm 10	2080 \pm 90	290 \pm 16

^a Cell volume is the mean value of measurements by two different methods (see "Materials and Methods").

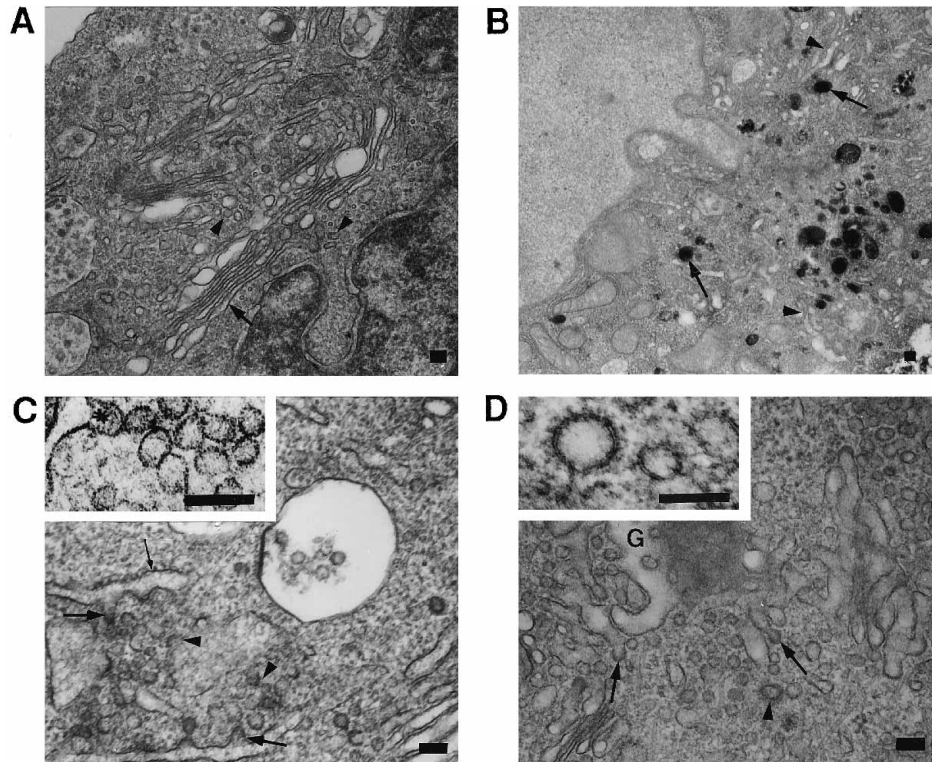
estimated with these two methods were 750 ± 34 and $810 \pm 41 \mu\text{m}^3$, respectively. The average of these two values ($780 \mu\text{m}^3$) was taken as a reliable estimate of RBL cell volume and was used to calculate all other morphometric parameters (see below and Table I).

The Golgi apparatus was defined as a complex of cisternae organized in stacks and tubular structures in the Golgi exclusion zone (Fig. 2A). In these areas, there may be two non-Golgi tubular structures: endosomes and transitional elements of the ER. The latter were excluded based on continuity with rough ER, presence of ribosomes on a contour, characteristic floccular content, and more abrupt membrane outline. Tubular endosomes were excluded based on their thinner diameter (40–50 instead of 60–90 nm for Golgi-associated tubules), very uniform width, and worm-like appearance; moreover, experiments designed to visualize the endosomal compartment by horseradish peroxidase staining showed that endosomes represent a negligible fraction of the membranes in the Golgi exclusion zone (Fig. 2B). Buds were defined as spherical-cylindrical elevations (diameter 60–100 nm) protruding from the surface of the ER (Fig. 2C) or of the Golgi complex (Fig. 2D) by at least 60% of their diameter, showing a direct connection with the donor membrane (ER or Golgi complex) and covered with electron-dense coats distinguishable from clathrin coats (Fig. 2D, *inset*). Vesicular profiles were defined as 50–80-nm round structures with a slightly denser content than that of Golgi cisternae. Given the high prevalence of vesicular (round) over tubular or oval profiles, we used the approximation that all round profiles represent vesicles, in order to calculate their number, surface, and volume. The tubular-vesicular clusters (TVC) derived from the ER (putative transport intermediates, see "Results") were defined as distinct aggregates of at least three vesicles adjacent to the ER or of at least two vesicles associated with an ER bud (Fig. 2C and *inset*). The average number of vesicular profiles in thin sections of such clusters was six.

To assess the volume and surface density (V_v and S_v , respectively) of the above defined structures, five random meshes on a grid, each containing at least 30 cell profiles from the same ultrasection, were used for each treatment and time point, photographed at $3000\times$, and photographically enlarged 14,000 times (to analyze whole cells), 31,120 times (for the ER), or 66,700 times (for the Golgi complex and TVC). The mean area (S_i) and perimeter (P_i) on thin sections of the above structures and of whole cells (S_c) was estimated with Videoplan 2, and V_v and S_v were calculated by the formulas: $V_v = S_i/S_c$ and $S_v = 2P_i/S_c$ (33). The number density (N_v) of buds, vesicles, and TVC in cells was estimated by the formula $N_v = C \cdot N_{3/2} \cdot V_v^{-1/2}$, where N_a is the mean number of profiles of these structures per cell sectional area and C is a constant related to their shape (33). Since these structures are rather spherical, we used a C coefficient equal to 1. The correction of bias due to section thickness and section compression was done according to Ref. 33. The correction factor for bud and vesicle number density was 0.41, as in Fig. 4 in Ref. 33. The correction factors for Golgi volume and surface were estimated as 0.6 and 0.64, respectively, based on Figs. 5 and 6 in Ref. 33 and on the reasonable assumption that two-thirds of the Golgi complex was composed of cisternae with an average length of 1 μm and one-third of tubules of 70 nm in diameter. The absolute values of surface (S_v), volume (V_v) and number (N_v) of the structures were calculated by the formulae $V_a = V_v \cdot \text{MCV}$, $S_a = S_v \cdot \text{MCV}$, and $N_a = N_v \cdot \text{MCV}$.

Cytochemistry—For horseradish peroxidase labeling of endosomal compartments, cells were incubated with 15 mg/ml horseradish peroxidase at 37 °C for 2 h, subjected to various treatments, and then washed with ice-cold PBS and fixed in 0.5% glutaraldehyde in 0.2 M sodium cacodylate, pH 7.4, for 30 min. Immediately after fixation, cells were washed with cacodylate buffer and reacted with diaminobenzidine for 1 min and then with diaminobenzidine and H_2O_2 for 30 min. The reaction was stopped by washing with cacodylate buffer; cells were then post-fixed in 2% OsO_4 , washed in sodium cacodylate, stained with 1% tannic acid for 1 h, and embedded in Epon. Sections (40–300 nm) were examined either at 60 or 80 kV in a Zeiss 109 transmission electron microscope.

FIG. 2. Ultrastructure of the components of the secretory pathway. A, a Golgi apparatus with membrane stacks (arrows), tubules, vesicles, and vacuoles (arrowheads). B, horseradish peroxidase labeling of early endosomes treated with 1 μ M PMA for 15 min and processed for cytochemical visualization of horseradish peroxidase (see "Experimental Procedures"). The horseradish peroxidase-labeled endosomes (arrows) were clearly distinct from the Golgi structure (arrowheads), and no horseradish peroxidase was detected in the Golgi area. C, ER-derived buds (arrows) and tubular-vesicular clusters (arrowheads and inset, asterisk) are situated near the ER (small arrows; see definitions in "Experimental Procedures"). D, tangential section of the Golgi cisternae (G) and buds therefrom (arrows). Clathrin-coated vesicles (arrowhead and inset) are distinguishable from non-clathrin-coated buds and vesicular profiles. Bars, 0.1 μ m.



RESULTS

We have studied the effects of membrane receptor stimulation on constitutive transport of soluble and membrane markers from TG/TGN to plasma membrane and on the morphology of the exocytic apparatus. Most experiments were carried out in RBL cells, where we had previously described the modulatory role of membrane receptors and PKC on ARF binding (14); other cell lines were employed to confirm and extend the results.

Constitutive GAG Release in RBL Cells—RBL cells are tumoral mastocytes and feature both constitutive and regulated secretion. It was thus important to assess whether a widely used assay of fluid-phase transport, the release of free [35 S]sulfate-labeled GAG (22) was an appropriate marker of constitutive secretion also in these cells. Preincubation of cells in xyloside-containing medium leads to the production of free soluble GAG since xyloside can substitute for the core proteins as the construction backbone for GAG synthesis. In particular, since sulfation of proteins and GAG occurs in the distal (TG/TGN) compartments of the Golgi complex in most cells (34, 35), the release of [35 S]sulfate-labeled GAG measures TG/TGN to plasma membrane transport. The composition of the 35 S-sulfated material synthesized by RBL cells in the presence of xyloside was analyzed by SDS-PAGE (22), and radioactivity was quantified with a Packard InstantImager (Fig. 3A). Fig. 3B shows how xyloside effectively induces GAG synthesis and correspondingly reduces endogenous proteoglycan synthesis, resulting in about 60% of total labeled molecular species being represented by low M_r GAG. Higher concentrations, or longer incubations, with xyloside increased further the levels of GAG (over the total incorporated radioactivity) but also caused cellular toxicity and were therefore not used. The time-course of constitutive proteoglycan and GAG release in RBL cells is shown in Fig. 3C. The $t_{1/2}$ of the process was approximately 30 min, and the maximal release at plateau (2 h) was about 40% of the total GAG content. The remaining 60% of the total 35 S-sulfated material remained associated with the cells even

after long chases. In mastocyte-type cells (among which are the RBL cells) a considerable amount of proteoglycans is stored in regulated secretory granules (Ref. 25 and references therein), suggesting that retained GAG might also be associated with the granule compartment. Fig. 3D shows how, after 6 h of chase, the vast majority (more than 70%) of the GAG remaining associated with RBL cells were released by stimuli typically effective on regulated secretory pools, indicating that it represents granule content.

Of note, proteoglycans (the high M_r sulfated material in Fig. 3A) appeared to behave similarly (although not identically) to GAG both in time course of secretion and responsiveness to stimulants (Fig. 3C) (experiments using various stimulants are described below). As GAG measurement involving SDS-PAGE and imaging is expensive and time consuming, we measured the release of sulfated material by cetylpyridinium chloride precipitation (a simpler technique that collectively detects GAG and proteoglycans, hereafter indicated as "glycans"), as an index of constitutive release. As expected, a good numerical correspondence was found between the two methods (for total glycans and GAG; Fig. 4). The cetylpyridinium chloride method was thus routinely used, and the SDS-PAGE/InstantImager technique was only employed to separately quantitate GAG and proteoglycans in selected experiments.

IgE Receptor Activation Stimulates Constitutive Glycan Release in RBL Cells Largely via PKC—The IgE receptor is the main activator of RBL cells. To study the effects of membrane receptor activation on constitutive release, RBL cells primed with anti-DNP monoclonal IgEs were preincubated with xyloside and pulse-labeled for 5 min with [35 S] sulfate to label glycans in the TG/TGN compartment. Cells were then treated with DNP-BSA in the absence of extracellular calcium, a condition known to completely abolish regulated secretion in these cells (Ref. 36 and this report). This increased the release of glycans by about 3–4-fold, but, as expected, it did not stimulate the regulated secretion of serotonin (Table II and Fig. 4A). The effect of the antigen on glycan secretion was completely inhib-

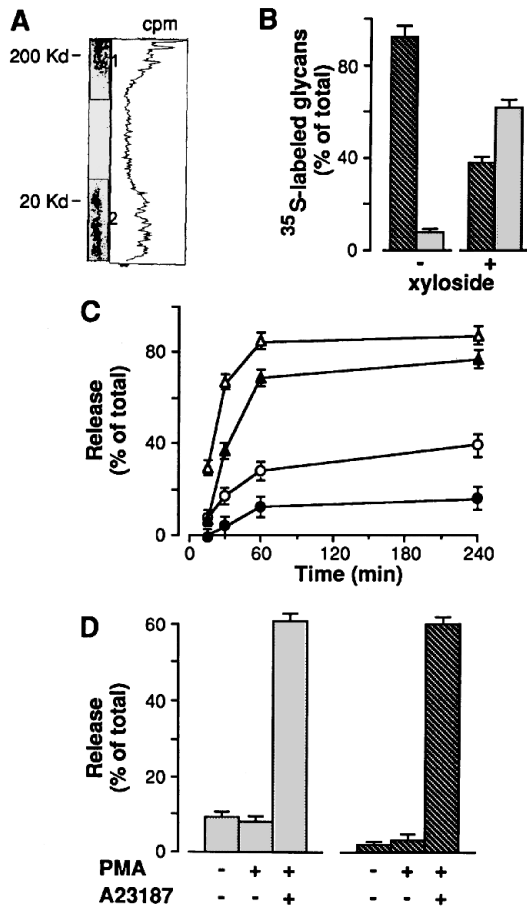


FIG. 3. Characterization of constitutive glycan release in RBL cells. Cells were pulse-labeled with [³⁵S]sulfate with or without preincubation in xyloside-containing medium. Total proteoglycans and GAG were separated by SDS-PAGE. A, sample image from the Packard InstantImager showing the separation between proteoglycans (1, high *M_r* material) and GAG (2, low *M_r* material), with the radioactivity profile. B, InstantImager quantification. In the graph, striped bars represent proteoglycans, and gray bars represent GAG. C, cells preincubated in the presence of xyloside and then pulse-labeled with [³⁵S]sulfate were chased for various times in the absence (circles) or presence of 100 nM PMA (triangles). Both content and released material were analyzed after SDS-PAGE separation by InstantImager quantification. Filled symbols represent proteoglycans, and empty symbols represent GAG. D, cells preincubated in xyloside and labeled as in B were chased for 6 h and then stimulated with 100 nM PMA with or without 1 μ M A23187 for 30 min. Content and released material were then analyzed after SDS-PAGE separation by InstantImager quantification. Striped bars represent proteoglycans, and gray bars represent GAG. Values represent means \pm S.D. Experiments were performed at least 3 times with similar results.

ited by 10 μ g/ml BFA (Fig. 4A). BFA did not affect the antigen-induced stimulation of serotonin release via the regulated pathway (when this was effected in the presence of extracellular calcium; Table II). The IgE receptor-coupled signal transduction machinery is complex and includes the phospholipase C-PKC cascade (37). In order to assess whether the receptor modulation of constitutive membrane transport was mediated by PKC, two specific PKC inhibitors (with two different binding sites on PKC, see below) were used: Ro 31-8220 and calphostin C. Fig. 4B shows how the stimulation of glycan release through IgE activation is largely, albeit not completely, inhibited by both inhibitors, indicating that PKC is involved in IgE receptor-activated glycan release. Both inhibitors were used at "specific" concentrations at which they had no effect on the stimulation of release induced by agents acting through protein kinase A or tyrosine kinases, in addition they did not appear to

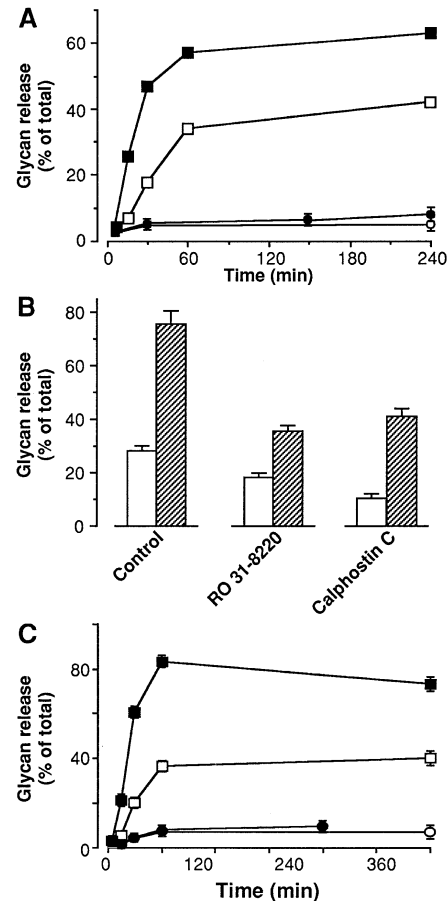


FIG. 4. Stimulation of constitutive glycan release by IgE receptor stimulation and by PMA in RBL cells. A, IgE-primed RBL cells were preincubated in the presence of xyloside, pulse-labeled with [³⁵S]sulfate, and then chased in calcium-free medium for 30 min in the presence (circles) or in the absence (squares) of 10 μ g/ml BFA, under basal conditions (empty symbols) or with 100 ng/ml DNP-BSA (filled symbols). B, IgE-primed RBL cells were treated as in A and then chased in calcium-free medium for 30 min in the absence (white bars) or in the presence of 100 ng/ml DNP-BSA (striped bars) and, where indicated, exposed to 5 μ M Ro 31-8220 or 1 μ M calphostin C. C, cells preincubated in the presence of xyloside and then pulse-labeled for 5 min with [³⁵S]sulfate were chased for various times with (filled symbols) or without (empty symbols) 100 nM PMA in the absence (squares) or presence (circles) of 10 μ g/ml BFA. Release was expressed as the percentage of the total cellular content as assayed by the cetylpyridinium chloride method. Values represent means \pm S.D. Experiments were performed at least 3 times with similar results.

be toxic at the practiced concentrations.² Moreover, an activator of PKC, the synthetic DAG analog PMA, mimicked the action of the IgE receptor. Fig. 4C shows the effects of 100 nM PMA added during the chase period. When cells were incubated at 19.5 $^{\circ}$ C for 1.5 h after the pulse to block labeled glycans in the distal Golgi, IgE receptor stimulation and direct stimulation of PKC both increased constitutive release (not shown), similar to the stimulation without the temperature block indicating direct acceleration of exit from the TG/TGN. Of note, the effect of PMA on GAG release was comparable with that on total glycan release evaluated by cetylpyridinium precipitation (confirming the equivalence of the two methods in assaying TGN to plasma membrane transport, see Figs. 3C and 4C).

While the above clearly suggests the involvement of PKC in

² R. Buccione, S. Bannykh, I. Santone, M. Baldassarre, F. Facchiano, Y. Bozzi, G. Di Tullio, A. Mironov, A. Luini, and M. A. De Matteis, unpublished observations.

TABLE II

Differential effects of activatory and inhibitory agents on constitutive and regulated release in RBL cells

For constitutive glycan release, cells preincubated in the presence of xyloside and then pulse labeled with [35 S]sulfate for 5 min were chased for 15 min in the presence or absence of 100 nM PMA with or without 10 μ M BFA. For IgE receptor stimulation IgE-primed cells were exposed to 100 ng/ml DNP-BSA with or without 10 μ M BFA. For regulated serotonin release [3 H]serotonin-loaded cells were stimulated in the presence or absence of 100 nM DNP-BSA, with or without 10 μ M BFA. All of the above was performed in the presence of 1.8 mM calcium with or without the addition of 3 mM EGTA to chelate all free calcium. Values represent means \pm S.D. Experiments were performed at least 3 times with similar results.

Treatment	Release (% of total \pm SD)			
	Ca $^{2+}$ -containing medium		Ca $^{2+}$ -deprived medium	
	Glycans	Serotonin	Glycans	Serotonin
Control	17.2 \pm 1.1	11.6 \pm 0.1	18.6 \pm 0.3	11.5 \pm 0.6
PMA	50.7 \pm 3.1	11.8 \pm 0.5	43.4 \pm 3.1	11.4 \pm 0.8
BFA	8.0 \pm 1.9	11.6 \pm 0.1	8.4 \pm 1.0	11.6 \pm 0.1
BFA/PMA	13.2 \pm 2.2	11.4 \pm 0.3	13.4 \pm 1.8	
DNP-BSA	58.3 \pm 3.4	63.3 \pm 0.1	43.6 \pm 2.9	10.5 \pm 0.2
DNP-BSA/BFA	14.7 \pm 0.1	69.7 \pm 1.1	9.7 \pm 0.2	

the regulation of constitutive exocytosis, it has been recently shown that a domain homologous to the phorbol ester binding region of PKC is present in other proteins (38, 39), raising the possibility that these proteins might be responsible for the stimulatory effects of PMA. A series of experiments was thus carried out to determine if the effect of PMA was due to PKC activation. Indeed, several other phorbol esters among which DPP, DPPA, and thymeleatoxin had a stimulatory effect on glycan release at concentrations shown to be active on purified PKC *in vitro* (Fig. 5A) (40); of notice, DPPA, which has been shown to exclusively stimulate β PKC *in vitro* (40) had the least effect on glycan release, being slightly effective only at the highest concentration (1 μ M). The inactive phorbol α -PDD had no effect (not shown). The specific PKC inhibitor calphostin C, which acts directly on the phorbol binding site of PKC (41), markedly reduced the stimulatory effect of PKC (Fig. 5B). Ro 31-8220, a highly specific PKC inhibitor acting at the ATP binding site of PKC (42), completely abolished the stimulatory effect of PMA (Fig. 5B). H7 and staurosporine, less selective compounds of the latter class, had similar effects (not shown). In addition, PMA was no longer able to stimulate glycan release after down-regulation of PKC with 1 μ M PMA treatment for 6 h (Fig. 5B). Calphostin C and Ro 31-8220 did not have effects on basal glycan release during the first 15 min after labeling, while an inhibition developed at later times (data not shown). The above results strongly suggest that PKC is responsible for the stimulatory effects of PMA on glycan release.

As noted above, RBL cells also feature regulated exocytosis and a considerable fraction of proteoglycans, and GAG (this report) accumulates in secretory granules. PMA alone does not stimulate release from secretory granules in RBL cells (Table II and Beaven *et al.* (36)), and, in addition, regulated secretion of serotonin was strictly dependent on external calcium, whereas PMA-stimulated glycan release was not. Finally, BFA did not inhibit serotonin release in clear contrast with its ability to inhibit glycan release. Thus, the pattern of responsiveness of the regulated secretory route in RBL cells to a variety of stimulators and inhibitors is completely different from that of the constitutive pathway. To further verify the separatedness of the two pathways, we followed the time-course of entry of GAG into the regulated compartment. After chases of increasing lengths, RBL cells were treated with PMA or DNP-BSA in the absence of extracellular calcium (to stimulate constitutive release) or a combination of calcium ionophore and PMA or DNP-BSA in the presence of external calcium (to induce regu-

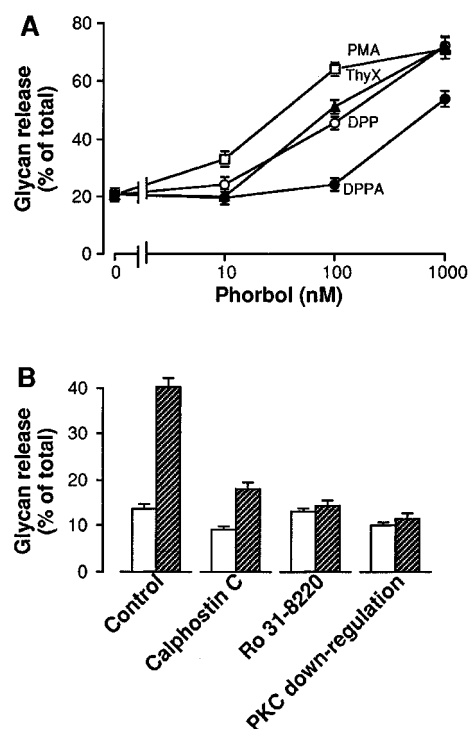


FIG. 5. Effects of specific stimulators and inhibitors of PKC on constitutive glycan release in RBL cells. A, cells preincubated in the presence of xyloside and then pulse-labeled with [35 S]sulfate were chased for 15 min in the presence of 10, 100, or 1000 nM PMA (squares), thymeleatoxin (triangles), DPP (empty circles), or DPPA (filled circles). Release was expressed as the percentage of the total cellular content as assayed by the cetylpyridinium chloride method. B, cells preincubated in the presence of xyloside and then pulse-labeled with [35 S]sulfate were chased for 15 min in the absence (white bars) or presence (striped bars) of 100 nM PMA together with 1 μ M calphostin C, 3 μ M Ro 31-8220, or, after 6 h of treatment, with 1 μ M PMA which down-regulates PKC isoforms α and β (71, 72). Release was expressed as above. Values represent means \pm S.D. Experiments were performed at least 3 times with similar results.

lated exocytosis, which is absolutely calcium-dependent in these cells; Ref. 36 and this report). When release was measured immediately after labeling, PMA (or DNP-BSA in the absence of calcium) potentially stimulated it. After 1 h of chase in the absence of stimuli, PMA moderately stimulated GAG release, whereas PMA/A23187 induced the release of about 60% of the total GAG content (not shown); the same was observed with IgE stimulation in the absence or the presence of external calcium, respectively. After 6 h of chase (Fig. 3D), PMA alone or IgE stimulation in the absence of external calcium (not shown) had no effect, whereas the vast majority of GAG content was released by PMA/A23187 or IgE stimulation in the presence of external calcium (not shown); the response to the latter stimuli precisely paralleled that seen with serotonin. This is taken to indicate that GAG had moved into a nonconstitutively releasing compartment, functionally colocalized with the serotonin-containing granule compartment. Thus, the kinetic data are in line with the other above results, indicating that in RBL cells, constitutive and regulated GAG secretion can be readily distinguished and that the former is selectively stimulated by PMA or by IgE receptor activation in the absence of calcium.

Effect of PKC Activators and Inhibitors on Transport of the VSV-G Protein from the TGN to the Plasma Membrane in RBL Cells—To determine whether the transport of a membrane-bound protein was also susceptible to regulation by PKC, we used the VSV-G (28), a widely accepted marker of membrane protein transport. Treatment with 100 nM PMA reproducibly increased the amount of VSV-G transported to the cell mem-

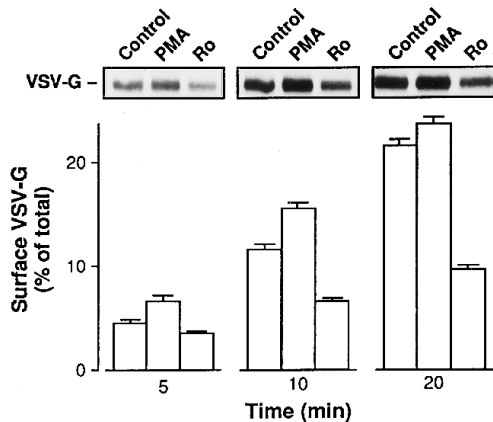


FIG. 6. Regulation of VSV-G transport from the TG/TGN to the cell surface in RBL cells. RBL cells, infected with VSV and labeled with [35 S]methionine were blocked at 19.5 °C to accumulate material in the TG/TGN. Cells were then chased at 37 °C in the presence or absence of 100 nM PMA or 5 μ M Ro 31-8220 (Ro). Biotinylated cell surface proteins were precipitated with streptavidin-agarose and quantified with the InstantImager after SDS-PAGE. Top panel shows the autoradiogram of a time-course of VSV-G transport to the cell surface. Bottom panel shows InstantImager quantification.

brane after an incubation at 19.5 °C to block material in the TGN, but the effect was quite small (up to about 30% over the control level). By contrast, the PKC inhibitor Ro 31-8220 profoundly and rapidly inhibited the basal rate of transport of VSV-G to the cell surface (Fig. 6). Therefore, like glycan transport, VSV-G traffic out of the TG/TGN appears to be regulated by PKC; however, the transport of the two markers and their regulation are different in their requirement for PKC activity, which appears to be crucial for stimulated but not basal constitutive glycan release, whereas the opposite seems to be true for VSV-G transport.

Effects of PMA on Secretory Vesicle Formation from the TG/TGN *In Vitro*—The effect of PKC activation was examined on the formation of vesicles from the TG/TGN in a cell-free system. RBL cells proved unsuitable for fractionation techniques aimed at producing a functioning TG/TGN. Many other cell types, including the pheochromocytoma-derived cell line PC12, polarized epithelial Madin-Darby canine kidney cells and the promyelocytic cell line HL-60, displayed a significant, albeit variable, stimulation of constitutive exocytosis in response to PMA (Fig. 7A). PC12 cells were thus used since they have been thoroughly characterized for use in assays of vesicle production *in vitro* from the TG/TGN (26). In detail, in these cells, after an initial delay of 2–3 min, the stimulatory effect of PMA peaked (to up to 200% of basal) between 5 and 15 min and declined thereafter (Fig. 7B). PMA affected the rate, but not the total amount, of glycan released at plateau. BFA was an extremely effective inhibitor of both basal and PMA-stimulated release (Fig. 7B). SDS-PAGE/InstantImager analysis showed that the great majority (80–90%) of released glycans was represented by low M_r GAG chains (not shown).

To measure vesicle production *in vitro*, PC12 cells were homogenized after a short pulse with [35 S]sulfate to produce a postnuclear supernatant containing, among other membranes, the Golgi complex. This postnuclear supernatant was incubated at 37 °C for various lengths of time in the presence or absence of 100 nM PMA or 10 μ M Ro 31-8220 and then fractionated by velocity gradient centrifugation to separate smaller secretory vesicles from larger TGN membranes between upper and lower fractions at 0 °C and 37 °C, according to Ref. 26 (see Fig. 1). The addition of PMA stimulated the transfer of labeled proteoglycans from lower (Golgi) into upper (vesicular) fractions (Table III). The inclusion of Ro 31-8220 during the incu-

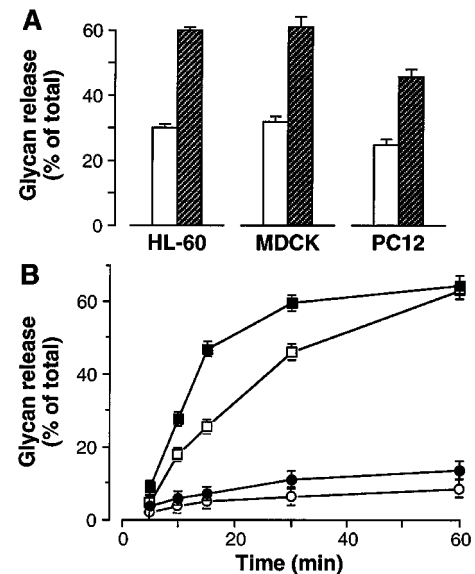


FIG. 7. Stimulation of glycan release by PMA in PC12 cells and other cell lines. A, HL-60, Madin-Darby canine kidney, and PC12 cells were preincubated in the presence of xyloside and then pulse-labeled with [35 S]sulfate and chased for 15 min with (striped bars), or without 100 nM PMA (white bars). B, PC12 cells, preincubated in the presence of xyloside and then pulse-labeled with [35 S]sulfate were chased for various times with (filled symbols) or without (empty symbols) 100 nM PMA in the absence (squares) or presence (circles) of 10 μ M BFA. Release was expressed as above. Values represent means \pm S.D., and experiments were performed at least 3 times with similar results.

TABLE III
Effect of PMA on cell-free formation of secretory vesicles from TG/TGN *in vitro* in PC12 cells

The ratio between radioactivity in the upper versus lower fractions represents an index of vesicle formation from the TG/TGN (see Fig. 1 for details). Values represent means \pm S.D. Experiments were performed 3 times with similar results.

Treatment	Vesicle formation (Ratio between cpm in upper and lower fractions)
0 °C	
Basal	0.41 \pm 0.15
PMA	0.38 \pm 0.16
37 °C	
Basal	0.87 \pm 0.22
PMA	1.43 \pm 0.21

bation inhibited vesicle formation (not shown). A similar increase in vesicle formation by PMA, albeit only in the presence of okadaic acid, was recently reported (11). These results indicate that PMA can increase vesicle formation and therefore that at least part of the acceleration of glycan release *in vivo* by PMA is due to a direct effect on export from the TG/TGN.

Effects of Plasma Membrane Receptor Stimulation and Direct PKC Activation on the Morphology of the Exocytic System—A series of morphometric analyses were carried out in RBL cells to examine whether relevant features of the secretory organelles might be quantitatively altered by IgE receptor activation and PMA stimulation. Under control conditions, the ER surface exhibited several coated buds that were often associated with TVC (see "Experimental Procedures"; possibly representing elements of the intermediate compartment) (45) whose main components were vesicular profiles of 60–65 nm in diameter. 11% of these buds were situated on the external surface of the nuclear envelope (Fig. 2C, inset). The Golgi complex also exhibited several coated buds (Fig. 2D) and was formed by 3.6 ± 0.1 stack profiles per cell; the number of cisternae per stack was 4.9 ± 0.2 .

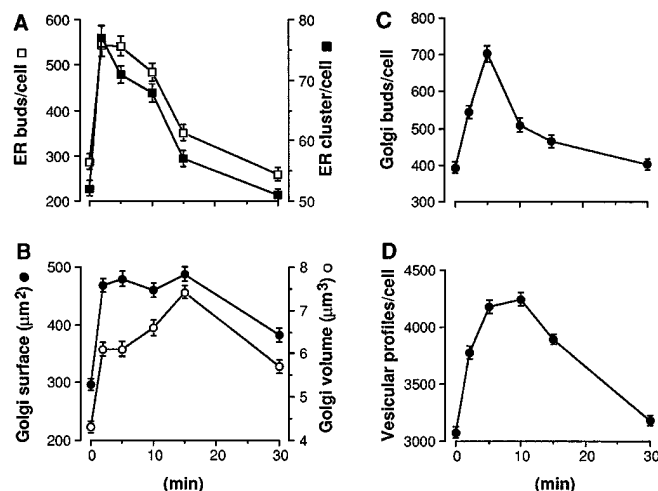


FIG. 8. Ultrastructural morphometric analysis of RBL cells stimulated with PMA. RBL cells were treated with 1 μ M PMA (which caused a stimulation of glycan release comparable with 100 nM PMA, see Fig. 5A) and then processed for morphometric analysis (see "Experimental Procedures"). A significant and rapid (2–15 min) increase of ER buds and TVC and a quick normalization of these parameters were observed (A). The number of Golgi buds and vesicles (C and D, respectively) increased to a slightly lesser degree. In a parallel manner, an increase of Golgi complex volume and surface (B) was observed.

When cells were treated with PMA, the number of buds on the ER increased by 90% within 2 min (Fig. 8A), while the distribution of the buds and the shape and size of the ER did not change appreciably. The number of ER-derived vesicular profiles and TVC rose to a somewhat lesser extent (Fig. 8A), while the number of vesicular profiles per TVC did not change. The number of total vesicular profiles was also significantly increased (Fig. 8D). Only less than half of this effect could be ascribed to ER vesicles; we did not attempt to determine the nature of the non-ER vesicular profiles, but they are likely to be mostly endocytic and Golgi-derived. A similar effect of PMA on cytoplasmic vesicles has been observed previously in human basophils (46). Concomitantly (within 2 min), the volume and surface of the Golgi apparatus increased by 40 and 55%, respectively (Fig. 8B), and the number of Golgi buds increased to a similar extent (Fig. 8C). The rims of Golgi profiles appeared to have become larger, and the number of Golgi profiles per cell appear to be slightly increased. The latter effect, however, might be due to increased probability of section through larger stacks rather than to an actual increase in stack profile number. Endocytosis in RBL cells can be stimulated by PMA (47); thus, to examine whether the changes attributed to the Golgi complex might in part be due to endocytic structures located in the Golgi area, cells were incubated with a high concentration of horseradish peroxidase (15 mg/ml) for 2 h to allow extensive labeling of the endosomal system. Several structures, mostly located in the cell periphery and identifiable as endosomes, became strongly horseradish peroxidase-labeled. In contrast, no horseradish peroxidase was detectable in the Golgi area both in control cells and in cells treated with PMA (Fig. 2B). Endosomes are thus unlikely to interfere with the identification of Golgi structures in RBL cells. Of note, these data also make it unlikely that stimulation of endocytosis by PMA might affect TG/TGN to plasma membrane traffic via an increased fluid input into the TG/TGN (see "Discussion"). At 10 min after PMA addition, the density of buds on the ER and the number of associated vesicular clusters began to decline; at 30 min of PMA treatment the number of ER buds and vesicular clusters had reached near basal levels (Fig. 8A). The Golgi complex also decreased in size, albeit with a delay, and began returning

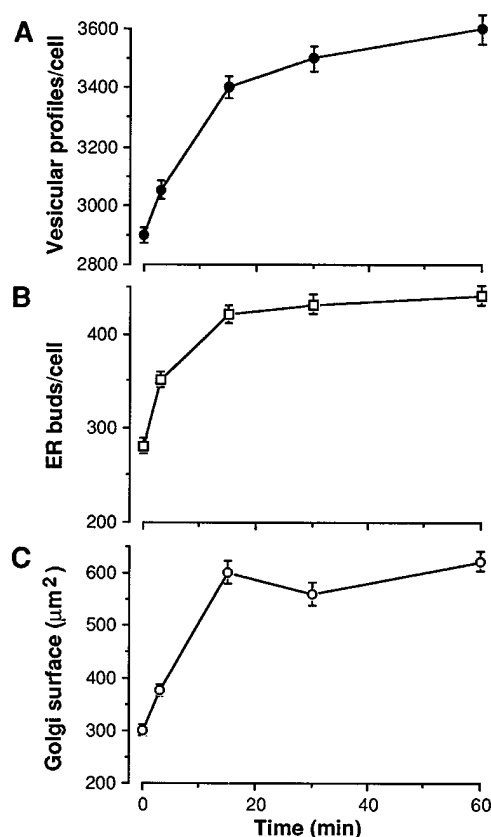


FIG. 9. Ultrastructural morphometric analysis after IgE receptor activation in RBL cells. IgE-primed cells were stimulated with 100 ng/ml DNP-BSA for different times and then processed for morphometry as described under "Experimental Procedures." The number of vesicles (A), ER buds (B), and the Golgi surface (C) rapidly increased reaching a plateau in about 20 min.

toward control values after 10–15 min of exposure to PMA (Fig. 8B). Treatments with PMA for up to 60 min had no significant effect on cell volume.

IgE receptor stimulation caused morphological effects similar to those of PMA. Indeed, receptor activation induced both an increase in number of ER buds and of associated vesicular clusters, and an enlargement of the Golgi complex (Fig. 9). These effects were slower to develop and less prominent than those of PMA but more prolonged in time, and they reached a maximal value after 60 min.

DISCUSSION

The Stimulation of Constitutive Transport by Plasma Membrane Receptors—This paper provides biochemical and morphometric evidence that the activation of the IgE receptor stimulates the constitutive exocytic pathway in RBL cells. PKC appears to be a key component in the transduction pathway mediating this response. This represents, to our knowledge, the first demonstration that a membrane receptor can activate exocytic membrane transport and concurrently induce rapid and profound morphological changes consistent with the functional activation.

The mechanism by which signals generated at the plasma membrane by the IgE receptor translocate to the transport apparatus is probably linked to the fact that IgE receptor activation stimulates the activity of soluble tyrosine kinases (48), which can, in turn, activate cytosolic phospholipase $C\gamma 1$ (49); PKC could thus be stimulated directly on the target organelle through the translocation of activated phospholipase $C\gamma 1$ and the consequent local production of DAG, the natural activator of the kinase. Very recently, we have found that other

receptors such as growth factor receptors, can stimulate constitutive secretion in a variety of cell lines, and that they can exert this effect even through PKC-independent mechanisms.² Thus, different signaling pathways appear to control constitutive traffic. To understand the physiological significance of these responses, it will be important to determine which types of receptors activate specific stations of the transport route and which second messengers are involved. It is likely that receptor-induced modulation of intracellular protein transport and sorting is involved in a variety of physiological phenomena. For instance, the stimulation of the membrane transport apparatus in mast cells via the IgE receptor might be required to prepare the complex recovery process that these cells must undergo after degranulation.

Analysis of the Role of PKC in the TG/TGN to Plasma Membrane Transport—The observations that, in RBL cells, the activation of IgE receptors generates DAG (49), and that PMA mimics the stimulatory effect of IgE receptor on constitutive transport from the TG/TGN to the plasma membrane obviously suggests that PKC is involved in receptor-induced activation of this traffic pathway. Moreover, we show that PKC activators stimulate constitutive exocytosis in a variety of cell types, indicating a remarkable generality of this phenomenon. It has recently been reported, however, that several proteins containing a domain homologous to the PMA/DAG binding region of PKC exist and may respond to PMA (38, 39, 50), suggesting the possibility that the IgE receptor- and PMA-induced regulation of constitutive traffic might be mediated by a protein(s) other than PKC. Moreover, a protein of this family has recently been implicated in maintaining the basal rate of ER to Golgi traffic (20). We provide several lines of evidence indicating that the IgE receptor and PMA effects on TG/TGN to plasma membrane traffic are mediated by PKC including that the effects of PMA and IgE receptors on transport were (a) mimicked only by phorbol esters active on PKC, (b) prevented by long PMA treatments inducing PKC down-regulation, and (c) suppressed not only by calphostin C, an inhibitor at the PMA/DAG binding site, but also by specific inhibitors acting at the catalytic site of the kinase. Therefore, both non-PKC PMA/DAG-binding protein(s) (20) and proteins of the PKC family (this study) seem to be able to exert regulatory effects on exocytic transport, a possibility that will have to be kept into account in future studies.

A relevant question concerning the role of PKC in constitutive release is whether the kinase can act directly on the TG/TGN to stimulate export toward the plasma membrane. In fact, in addition to the ER to Golgi traffic segment (20), endocytosis (19, 51) and apical endosome-plasma membrane recycling in polarized cells (16) have been reported to be stimulated by PMA. It is thus possible that the stimulation of TG/TGN to plasma membrane transport might be due to enhanced membrane flow in other districts of the cell rather than a direct activation of export from the TG/TGN. For instance, the stimulation of endocytosis and ER to Golgi transport could increase the input of surface and volume into the TG/TGN, thereby stimulating a compensatory output from it. However, the demonstration, in PC12 cells, that PMA accelerates the formation of proteoglycan-containing vesicles from cell-free TG/TGN preparations (where such indirect effects are very unlikely to occur) indicates that at least part of the effect of PMA on glycan release is due to a direct action on the TG/TGN. It should be noted, at the same time, that this experiment does not exclude the possibility that other (indirect) effects of PMA may occur *in vivo*, especially because the effect observed in cell-free vesicle formation experiments is smaller than the overall acceleration of glycan release seen in intact cells (it is also possible, how-

ever, that this discrepancy may simply be due to a lower efficiency of the *in vitro* reaction). Further support for a direct action of PMA on the TG/TGN comes from a different set of experiments in intact RBL cells, showing that there is no detectable input from the endocytic pathway into the TG/TGN (see Fig. 2) and that, after a prolonged temperature block at 19.5 °C, IgE receptor and PKC activation strongly accelerate exit from the TG/TGN. In conclusion, the collective data indicate that the stimulatory action of PMA on TG/TGN to plasma membrane transport is, at least in part, due to a direct activation of membrane export from the TG/TGN.

Another question concerns the differential roles of PKC in the transport of fluid-phase and membrane markers, since the transport of GAG (a fluid-phase marker) was potentially accelerated by PKC activators, whereas the transport of VSV-G (a membrane protein) was rapidly and markedly inhibited by PKC inhibitors (compare Figs. 4 and 6). A difficulty in interpreting these results is that the appearance of membrane markers on the plasma membrane depends on the balance between exocytic and endocytic activities, whereas the release of soluble molecules is mainly due to exocytic transport. Nevertheless, it seems to us that the most economical explanation of the results may be based on recent reports that soluble and membrane proteins are transported to the plasma membrane in distinct vesicular carriers (43, 44). Another alternative explanation is based on the fact that, in RBL cells, a large amount of soluble glycans are eventually accumulated in secretory granule, which would occur via intermediates generally referred to as "immature granule." Constitutive exit from this compartment has clearly been shown (for a review, see Ref. 52), and it is thus possible that PKC and receptor activation might accelerate this constitutive-like (*i.e.* not calcium-dependent) transport toward the plasma membrane. Thus, if indeed there are different transport mechanisms for GAG and VSV-G, they might be differentially regulated by PKC.

Mechanisms of Activation and Targets of the PKC Isoform(s) Involved in Regulating Membrane Traffic—As mentioned above, a likely mechanism through which IgE receptors exert their control on membrane traffic is the induction of increased DAG levels in the TG/TGN (as well as presumably in other stations of the traffic pathways), and the consequent local activation of a PKC isoform(s). PMA could mimic the receptor-induced effects by directly activating PKC at the same intracellular sites. In connection with this, it is interesting to note that DAG can be formed not only in response to receptor stimulation but also (at least in the ER and the Golgi complex) during lipid metabolic reactions (53); in addition, several heterotrimeric G proteins that activate DAG-forming enzymes such as phospholipases C in "canonical" transduction pathways are located on intracellular organelles including the ER and the Golgi complex (2, 54). It is thus conceivable that DAG may not only be a direct mediator of secretory responses to receptor activation but also that DAG levels (and, consequently, PKC activity) in secretory organelles (controlled either by lipid metabolic pathways or by "local" G proteins; see Ref. 55 and discussion below) may play a significant role in determining basal traffic rates (53, 56).

What is the target of PKC in the traffic machinery? A good candidate is the mechanism of ARF activation and/or binding to Golgi membranes, since this is a key event in vesicle formation already known to be modulated by PKC (14). The involvement of ARF in promoting the assembly of different kinds of coat onto Golgi membranes, is indicated both by direct evidence and by the use of BFA that blocks the activation of ARF (7, 57, 58). With regard to the TG/TGN, BFA is known to block constitutive transport from the TG/TGN to the plasma membrane

(59) (this report); moreover, ARF has also been found to be associated with proteoglycan-carrying post-TGN vesicles in rat hepatocytes (42). Other targets of PKC in the traffic machinery cannot be excluded. For instance, the phospholipase D-stimulating activity of ARF (60, 61) has been recently shown to be potentiated by PMA in human neutrophils (62).

The identity and the localization of the PKC isoform(s) that controls membrane traffic is presently unclear. PKC is part of a family of several isozymes with different sensitivities to modulators and substrate specificities (63, 64). The α , β , and ϵ isoforms have previously been hypothesized to be involved in the regulation of membrane traffic (14, 16, 19, 65). A series of experiments in COS 7 cells, which normally express these isoforms and respond to PMA with an increase in glycan secretion have, however, revealed that these kinases are not involved in regulating membrane traffic (at least in these cells). In fact, when α - and β -PKC were overexpressed together with the secretory mutant of human alkaline phosphatase (66), neither the basal secretion rate of the secretory mutant of human alkaline phosphatase nor the potency of PMA in eliciting the secretory response appeared to change,² as one would have expected if the overexpressed isoforms had been involved in the PMA stimulation of membrane traffic (67, 68). Interestingly when the ϵ isoform was overexpressed, the response to PMA was completely lost² in accordance with a recent report (65). More work using the co-transfection approach employed in this study will be necessary to identify the relevant PKC isoform(s).

Significance of the Morphological and Functional Changes in the Exocytic Pathway Induced by IgE Receptor and PKC Stimulation—The morphometric data, combined with the activatory effect of IgE receptors and PMA on secretory traffic shown in this study, together with the recent finding that PMA strongly (4-fold) stimulates ER to Golgi transport (20), suggest a picture consistent with a regulatory role of PKC (and other PMA-binding proteins) on the entire secretory pathway. The simplest interpretation of the observed increase in the number of ER buds and ER-derived vesicles accompanied by a transient increase in surface and volume of the Golgi complex (Fig. 8) is that PMA enhances the probability of budding and vesicle formation from the ER, thereby driving an accelerated flow of membrane into the Golgi (20) and causing the consequent rapid increase of the organelle's size. Moreover, the increase in number of Golgi buds and total vesicular profiles is consistent with the acceleration in exocytic export from the TG/TGN induced by PKC stimulation.³ These conclusions are in agreement with a comprehensive study of the morphological effects of PMA on transport organelles.⁴

If one makes the reasonable assumption that the increase in Golgi size (60% in 2 min) is mostly due to enhanced membrane input from the ER, one obtains that the observed PMA-induced Golgi increase requires an acceleration in net membrane transport from the ER to the Golgi corresponding to at least 5% of the ER surface/min. Clearly this effect, if continued, would rapidly lead to gross imbalances in the sizes of the secretory organelles. Similar considerations can be made based on func-

tional (GAG release) data, with respect to the TG/TGN. The half-time of GAG release from the cell lines here used ranges from 15 to 30 min; these estimations, assuming that GAG are homogenous markers of the TG/TGN luminal space, would also reflect the half-time of turnover of this organelle. If so, a 100% increase in export rate from the TG/TGN such as that described here would, again, lead to substantial changes in the size of the organelle within a short time if homeostatic mechanisms were not in place.

Thus, this study introduces a novel appreciation of the rapidity and extent of the variations in membrane traffic rates that may occur under physiological conditions and supports the notion that there must be ways in which traffic movements in different organelles are precisely matched to preserve the "homeostasis" of cell membranes. While this idea has occasionally surfaced in the literature, the mechanisms presiding over such fine regulation have not been investigated. One possibility that may now be suggested is that DAG or other second messengers (see recent data implicating cAMP in the regulation of transcytosis and endocytosis) (17, 18, 19) may be involved not only in mediating the variations in traffic rates induced by a membrane receptor, as shown here, but also in restoring, when necessary, "normal" conditions in the secretory pathway. It is possible, for instance, that individual organelles may possess sensors for excessive changes in their size and shape that would generate messengers to re-establish "correct" functioning status. The heterotrimeric G proteins located on secretory organelles might play a role in these intracellular signaling systems functioning in and between organelles (55). Interestingly, an example of interorganelle signaling (albeit apparently not involving G proteins) has been recently provided by the finding that events in the lumen of the ER can be sensed and signaled via a protein kinase to the nucleus, to control the transcription of ER chaperon proteins (69, 70). A variety of transduction signals may be used as one of the mechanisms functioning to maintain the homeostasis of intracellular traffic pathways and to mediate their adaptive responses to receptor stimuli.

Acknowledgments—We thank Drs. G. Griffiths and R. Parton for critical discussion of the morphometric data.

REFERENCES

- Rothman, J. E. (1994) *Nature* **372**, 55–63
- Stow, J. L., de Almeida, J. B., Narula, N., Holtzman, E. J., Ercolani, L., and Ausiello, D. A. (1991) *J. Cell Biol.* **114**, 1113–1124
- Pimplikar, S. W., and Simons, K. (1993) *Nature* **362**, 456–458
- Colombo, M. L., Mayorga, L. S., Casey, P. J., and Stahl, P. D. (1992) *Science* **255**, 1695–1697
- Bomsel, M., and Mostov, K. E. (1993) *J. Biol. Chem.* **268**, 25824–25835
- Barroso, M., and Sztul, E. S. (1994) *J. Cell Biol.* **124**, 83–100
- Donaldson, J. G., Kahn, R. A., Lippincott-Schwartz, J., and Klausner, R. D. (1991) *Science* **254**, 1197–1199
- Barr, F. A., Leyte, A., Mollner, S., Pfeuffer, T., Tooze, S. A., and Huttner, W. B. (1991) *FEBS Lett.* **294**, 239–243
- Schwaninger, R., Plutner, H., Bokoch, G. M., and Balch, W. E. (1992) *J. Cell Biol.* **119**, 1077–1096
- Davidson, H. W., McGowan, C. H., and Balch, W. E. (1992) *J. Cell Biol.* **116**, 1343–1355
- Ohashi, M., and Huttner, W. B. (1994) *J. Biol. Chem.* **269**, 24897–24905
- Woodman, P. G., Mundy, D. I., Cohen, P., and Warren, G. (1992) *J. Cell Biol.* **116**, 331–338
- Tuomikoski, T., Felix, M. A., Doree, M., and Gruenberg, J. (1989) *Nature* **342**, 942–945
- De Matteis, M. A., Santini, G., Kahn, R. A., Di Tullio, G., and Luini, A. (1993) *Nature* **364**, 818–821
- Luini, A., and De Matteis, M. A. (1993) *Trends Cell Biol.* **3**, 290–292
- Cardone, M. H., Smith, B. L., Song, W., Mochly-Rosen, D., and Mostov, K. E. (1994) *J. Cell Biol.* **124**, 717–727
- Hansen, S. H., and Casanova, J. E. (1994) *J. Cell Biol.* **126**, 677–687
- Pimplikar, S. W., and Simons, K. (1994) *J. Biol. Chem.* **269**, 19054–19059
- Eker, P., Holm, P. K., van Deurs, B., and Sandvig, K. (1994) *J. Biol. Chem.* **269**, 18607–18615
- Fabbri, M., Bannykh, S., and Balch, W. E. (1994) *J. Biol. Chem.* **269**, 26848–26857
- Turner, M. D., Wilde, C. J., and Burgoyne, R. D. (1992) *Biochem. J.* **286**, 13–15
- Brion, C., Miller, S. G., and Moore, H.-P. H. (1992) *J. Biol. Chem.* **267**,

³ Combining morphometric and transport data, one might expect, based on the effect on GAG release and on the $t_{1/2}$ of release of GAG (considered as a marker of TG/TGN bulk volume; Figs. 2 and 3), a decrease in size of the TG/TGN within the first several minutes of PMA treatment. However, while this decrease might in fact occur, it would be undetectable for technical reasons, since in our experiments the tubular structures of the TG/TGN cannot be reliably distinguished from the cis Golgi tubules. Instead, since all Golgi elements are recorded together for quantitative estimations, the possible membrane loss from the TG/TGN is more than counterbalanced by the increased input into the cis Golgi from the ER, whose size is 5–10-fold larger than that of the Golgi complex (Table I).

⁴ S. Bannykh and W. Balch, personal communication.

- 1477–1483
23. Laemmli, U. K. (1970) *Nature*. **227**, 680–685
24. Miller, S. G., Carnell, L., and Moore, H.-P. H. (1992) *J. Cell Biol.* **118**, 267–283
25. De Matteis, M. A., Di Tullio, G., Buccione, R., and Luini, A. (1991) *J. Biol. Chem.* **266**, 10452–10460
26. Toozé, S. A., and Huttner, W. B. (1992) *Methods Enzymol.* **219**, 81–93
27. Brändli, A. W., Hansson, G. C., Rodriguez-Boulán, E., and Simons, K. (1988) *J. Biol. Chem.* **263**, 16283–16290
28. Bergmann, J. E. (1989) *Methods Cell Biol.* **32**, 85–110
29. Linstedt, A. D., and Kelly, R. B. (1991) *Neuron* **7**, 309–317
30. Le Bivic, A., Sambuy, Y., Mostov, K., and Rodriguez-Boulán, E. (1990) *J. Cell Biol.* **110**, 1533–1539
31. Baddeley, A. J., Gundersen, H. J. G., and Cruz-Orive, L. M. (1986) *J. Microsc. (Oxf.)* **142**, 259–276
32. Griffiths, G., Fuller, S. D., Back, R., Hollinshead, M., Pfeiffer, S., and Simons, K. (1989) *J. Cell Biol.* **108**, 277–297
33. Weibel, E. R. (1979) *Stereological Methods: Vol. I. Practical Methods for Biological Morphometry*, Academic Press, New York
34. Baeuerle, P. A., and Huttner, W. B. (1987) *J. Cell Biol.* **105**, 2655–2664
35. Graham, J. M., and Winterbourne, D. J. (1988) *Biochem. J.* **252**, 437–445
36. Beaven, M. A., Guthrie, D. F., Moore, J. P., Smith, G. A., Hesketh, T. R., and Metcalfe, J. C. (1987) *J. Cell Biol.* **105**, 1129–1136
37. Beaven, M. A., and Metzger, H. (1993) *Immunol. Today* **14**, 222–226
38. Ahmed, S., Kozma, R., Monfries, C., Hall, C., H., Lim, L., Smith, P., and Lim, L. (1990) *Biochem. J.* **272**, 767–773
39. Ahmed, S., Kozma, R., Lee, J., Monfries, C., Harden, N., and Lim, L. (1991) *Biochem. J.* **280**, 233–241
40. Ryves, W. J., Evans, A. T., Olivier, A. R., Parker, P. J., and Evans, F. J. (1991) *FEBS Lett.* **288**, 5–9
41. Kobayashi, E., Nakano, H., Morimoto, M., and Tamaoki, T. (1989) *Biochem. Biophys. Res. Commun.* **159**, 548–553
42. Twomey, B., Muid, R. E., Nixon, J. S., Sedgwick, A. D., Wilkinson, S. E., and Dale, M. M. (1990) *Biochem. Biophys. Res. Commun.* **171**, 1087–1092
43. Nickel, W., Huber, L. A., Kahn, R. A., Kipper, N., Barthel, A., Fasshauer, D., and Söling, H.-D. (1994) *J. Cell Biol.* **125**, 721–732
44. Saucan, L., and Palade, G. E. (1994) *J. Cell Biol.* **125**, 733–741
45. Lotti, L. V., Torrisi, M.-R., Pascale, M. C., and Bonatti, S. (1992) *J. Cell Biol.* **118**, 43–50
46. Dvorak, A. M., Warren, J. A., Morgan, E., Kissell-Rainville, S., Lichtenstein, L. M., and MacGlashan, D. W. (1992) *Am. J. Pathol.* **141**, 1309–1322
47. Pfeiffer, J. R., Seagrave, J. C., Davis, B. H., Deanin, G. G., and Oliver, J. M. (1985) *J. Cell Biol.* **101**, 2145–2155
48. Yu, K.-T., Lyall, R., Jariwala, N., Zilberstein, A., and Haimovich, J. (1991) *J. Biol. Chem.* **266**, 22564–22568
49. Park, D. J., Min, H. K., and Rhee, S. G. (1991) *J. Biol. Chem.* **266**, 24237–24240
50. Kazanietz, M. G., Bustelo, X. R., Barbacid, M., Kolch, W., Mischak, H., Wong, G., Pettit, G. R., Bruns, J. D., and Blumberg, P. M. (1994) *J. Biol. Chem.* **269**, 11590–11594
51. Swanson, J. A., Yirinec, B. D., and Silverstein, S. C. (1985) *J. Cell Biol.* **100**, 851–859
52. Arvan, P., and Castle, J. D. (1992) *Trends Cell Biol.* **2**, 327–331
53. Pagano, R. E. (1988) *Trends Biochem. Sci.* **13**, 202–205
54. Wilson, B. G., Komuro, M., and Gist Farquhar, M. (1994) *Endocrinology* **134**, 233–244
55. Bomsel, M., and Mostov, K. E. (1992) *Mol. Biol. Cell* **3**, 1317–1328
56. McGee, T. P., Skinner, H. B., Whitters, E. A., Henry, S. A., and Bankaitis, V. A. (1994) *J. Cell Biol.* **124**, 273–287
57. Stamnes, M. A., and Rothman, J. E. (1993) *Cell* **73**, 999–1005
58. Narula, N., McMorro, I., Plopper, G., Doherty, J., Matlin, K. S., Burke, B., and Stow, J. L. (1992) *J. Cell Biol.* **117**, 27–38
59. Rosa, P., Barr, F. A., Stinchcombe, J. C., Binacchi, C., and Huttner, W. B. (1992) *Eur. J. Cell Biol.* **59**, 265–274
60. Brown, H. A., Gutowski, S., Moomaw, C. R., Slaughter, C., and Sternweis, P. C. (1993) *Cell* **75**, 1137–1144
61. Cockcroft, S., Thomas, G. M. H., Fensome, A., Geny, B., Cunningham, E., Gout, I., Hiles, I., Totty, N. F., Truong, O., and Hsuan, J. J. (1994) *Science*. **263**, 523–526
62. Whatmore, J., Cronin, P., and Cockcroft, S. (1994) *FEBS Lett.* **352**, 113–117
63. Hug, H., and Sarre, T. F. (1993) *Biochem. J.* **291**, 329–343
64. Kazanietz, M. G., Areces, L. B., Bahador, A., Mischak, H., Goodnight, J., Mushinski, J. F., and Blumberg, P. M. (1993) *Mol. Pharmacol.* **44**, 298–307
65. Lehel, C., Olah, Z., Jakab, G., and Anderson, W. B. (1995) *Proc. Natl. Acad. Sci. U. S. A.* **92**, 1406–1410
66. Berger, J., Hauber, J., Hauber, R., Geiger, R., and Cullen, B. R. (1988) *Gene (Amst.)* **66**, 1–10
67. Slack, B. E., Nitsch, R. M., Livneh, E., Kunz, G. M., Jr., Breu, J., Eldar, H., and Wurtman, R. J. (1993) *J. Biol. Chem.* **268**, 21097–21101
68. Akita, Y., Ohno, S., Yajima, Y., Konno, Y., Saido, T. C., Mizuno, K., Chida, K., Osada, S., Kuroki, T., Kawashima, S., and Suzuki, K. (1994) *J. Biol. Chem.* **269**, 4653–4660
69. Cox, J. S., Shamu, C. E., and Walter, P. (1993) *Cell*. **73**, 1197–1206
70. Mori, K., Ma, W., Gething, M. J., and Sambrook, J. (1993) *Cell* **74**, 743–756
71. Ozawa, K., Szallasi, Z., Kazanietz, M. G., Blumberg, P. M., Mischak, H., Mushinski, J. F., and Beaven, M. A. (1993) *J. Biol. Chem.* **268**, 1749–1756
72. Buccione, R., Di Tullio, G., Caretta, M., Marinetti, M. R., Bizzarri, C., Francavilla, S., Luini, A., and De Matteis, M. A. (1994) *Biochem. J.* **298**, 149–156